were the points of comparisons; 1) sensitivity to grid quality and 2) effect of artificial dissipation.

The two methods were stable and equally accurate with uniform grid. The finite element method was found to be less sensitive to grid nonuniformity for the cases considered. Finally, the FEM and FVM required approximately the same amount of computing time per cell per step. However, the amount of required memory storage was more than double for the FEM.

Acknowledgment

This work is supported by the NSF Engineering Research Centers program Grant CDR-8721512.

References

[1]Kallinderis, Y., and Nakajima, K., "A Finite-Element Method for the Incompressible Navier-Stokes Equations with Adaptive Hybrid Grids," AIAA Paper 93-3005, July 1993.

[2]Nakajima, K., "Incompressible Navier-Stokes Methods with Hybrid Adaptive Grids," M. S. Thesis, Dept. of Aerospace Engineering and Engineering Mechanics, Univ. of Texas at Austin, TX, May 1993.

Practical Formulation of a Positively Conservative Scheme

Shigeru Obayashi*
NASA Ames Research Center, Moffett Field, California 94035
and
Yasuhiro Wada†
NASA Lewis Research Center, Cleveland, Ohio 44135

Introduction

APPROXIMATE Riemann solvers have been highly successful for computing the Euler/Navier-Stokes equations, but linearized Riemann solvers are known to fail occasionally by predicting non-physical states with negative density or internal energy. Positively conservative schemes, in contrast, guarantee physical solutions from realistic input. The Harten-Lax-van Leer-Einfeldt (HLLE) scheme is a typical example of a positively conservative scheme.[1] However, the HLLE scheme is highly dissipative at contact discontinuities and shear layers and thus it is not applicable to practical simulations. An existing modification to the HLLE scheme, known as HLLEM, enhances the resolution to that of the Roe scheme.[2] However, this modification violates the positivity of density and internal energy. Precise derivation of the modification yields a quadratic inequality and thus requires a case-by-case treatment.[3] This Note describes a new, modified HLLE scheme that satisfies the positively conservative condition approximately. Sample computations are included to demonstrate the resolution and the robustness of the scheme.

Algorithm Development

For brevity, the Euler equations are limited to one Cartesian space dimension. The conservation form of the equation is

$$Q_t + F_x = 0 \tag{1a}$$

where the conserved quantities Q and flux F are

$$Q = \begin{pmatrix} \rho \\ \rho u \\ e \end{pmatrix}, \qquad F = \begin{pmatrix} \rho u \\ \rho u^2 + p \\ (e+p)\,u \end{pmatrix} \tag{1b}$$

and where ρ is the density, u is the velocity, and e is the total energy per unit volume. The pressure p is related to the conserved quantities through the equation of state for a perfect gas:

$$p = (\gamma - 1)(e - \rho u^2/2) \tag{1c}$$

The cell interface flux F_{LR} can be evaluated by the HLLE scheme[1] as

$$F_{LR} = 1/2(F_L + F_R - \bar{R}\hat{\Lambda}\bar{L}\Delta Q) \tag{2a}$$

where

$$\Delta Q = Q_R - Q_L \tag{2b}$$

$$\hat{\Lambda} = (b_R^+ + b_L^-)/(b_R^+ - b_L^-)\,\bar{\Lambda} - 2(b_R^+ b_L^-)/(b_R^+ - b_L^-)I \tag{2c}$$

$$\bar{\Lambda} = \begin{pmatrix} \bar{u} & & 0 \\ & \bar{u} + \bar{c} & \\ 0 & & \bar{u} - \bar{c} \end{pmatrix} \tag{2d}$$

and where $\bar{R}$, $\bar{\Lambda}$, and $\bar{L}$ are the right eigenvector, eigenvalue, and left eigenvector matrices, respectively, of the Roe-averaged Jacobian,[4] I is the identity matrix, and the subscripts L and R indicate the left and right states. The HLLE scheme defines b_R^+ and b_L^- as

$$b_R^+ = \max(\bar{u} + \bar{c}, u_R + c_R, 0) \tag{3a}$$

$$b_L^- = \min(\bar{u} - \bar{c}, u_L - c_L, 0) \tag{3b}$$

This scheme satisfies all of the stability, entropy, and positively conservative conditions required for the nonlinear difference equations.[1-3] Numerical dissipation determined by b_R^+ and b_L^- could still be reduced under the stability and positively conservative conditions.[1] However, the resulting scheme would violate the entropy condition[3] and thus it is not used here.

The HLLE scheme approximates the solution of the Riemann problem with two waves propagating with speed of $b_R = \max(\bar{u} + \bar{c}, u_R + c_R)$ and $b_L^- = \min(\bar{u} - \bar{c}, u_L - c_L)$ and a state Q_{LR} between those waves. Comparing with the Roe scheme, the HLLE scheme introduces large numerical dissipation to contact discontinuities.[1] The modified HLLE (HLLEM) scheme exhibits a similar resolution to the Roe scheme,[1] but the resulting scheme violates the positively conservative condition.[3] A new modification[3] which satisfies the positively conservative condition is obtained by replacing the state Q_{LR} with

$$\tilde{Q}_{LR} = \begin{cases} Q_{LR} - \delta\bar{B}\Delta Q, & \text{for } x/t < (b_L + b_R)/2 \\ Q_{LR} + \delta\bar{B}\Delta Q, & \text{for } x/t > (b_L + b_R)/2 \end{cases} \tag{4a}$$

where

$$Q_{LR} = [b_R Q_R - b_L Q_L - (F_R - F_L)]/(b_R - b_L) \tag{4b}$$

and

$$\bar{B}\Delta Q = \bar{R}\begin{pmatrix} 1 & & \\ & 0 & \\ & & 0 \end{pmatrix}\bar{L}\Delta Q = \frac{\bar{c}^2\Delta\rho - \Delta p}{\bar{c}^2}\begin{pmatrix} 1 \\ \bar{u} \\ \bar{u}^2/2 \end{pmatrix} \tag{4c}$$

Received Aug. 31, 1993; accepted for publication Oct. 13, 1993.

*Senior Research Scientist, MCAT Institute. Senior Member AIAA.

†Institute for Computational Mechanics in Propulsion; currently at Computational Sciences Division, National Aerospace Laboratory, Tokyo, Japan. Member AIAA.

The cell interface flux is obtained by replacing $\hat{\Lambda} = \text{diag}\,[\hat{\lambda}_1, \hat{\lambda}_2, \hat{\lambda}_3]$ in Eq. (2a) with

$$\tilde{\Lambda} = \text{diag}\,[\hat{\lambda}_1 - 2\delta \min(b_R^+, b_L^-), \hat{\lambda}_2, \hat{\lambda}_3] \tag{5}$$

where $0 < \delta < 1/2$ from the stability condition. The resulting scheme becomes identical to the Roe scheme when $\delta = 1/2$, and to the HLLE scheme when $\delta = 0$. From the positively conservative condition for density, $\tilde{\rho}_{LR} > 0$, one obtains $\rho_{LR} \pm \delta\sigma_1 > 0$ where $\sigma_1 = \Delta\rho - \Delta p/\bar{c}_2$; thus,

$$\delta < \frac{\rho_{LR}}{|\sigma_1|} \tag{6}$$

From the positively conservative condition for internal energy, one also obtains

$$e_{LR} \pm \delta\sigma_1 \frac{\bar{u}^2}{2} - \frac{\rho_{LR} u_{LR} \pm \delta\sigma_1 \bar{u}^2}{2\rho_{LR} \pm \delta\sigma_1} > 0 \tag{7}$$

Since $\rho_{LR} \pm \delta\sigma_1 > 0$, this inequality results in

$$\rho_{LR}\left(e_{LR} - \frac{\rho_{LR} u_{LR}^2}{2}\right) \pm \delta\sigma_1 \left\{e_{LR} - \frac{\rho_{LR} u_{LR}^2}{2} + \frac{\rho_{LR}}{2}(u_{LR} - \bar{u})^2\right\} > 0 \tag{8}$$

Note that the coefficient of the δ^2 term cancels out for a perfect gas in the one-dimensional case. For the multidimensional case or the nonequilibrium gas case, the coefficient of the δ^2 term does not cancel and the quadratic inequality has to be solved as described in Ref. 3. However, when the space increment is h, the coefficient remains of $\mathcal{O}(h^2)$ for those cases. Therefore, inequality (8) is still valid within the error of $\mathcal{O}(h^2)$. Suppose $b_R = u_R + c_R$ and $b_L = u_L - c_L$, from Eq. (4b), one obtains

$$u_{LR} = [c_R \rho_R u_R + c_L \rho_L u_L - (p_R - p_L)]/(c_R \rho_R + c_L \rho_L) \tag{9}$$

Thus,

$$u_{LR} = \bar{u} - (\Delta p/2\bar{\rho}\bar{c}) + \mathcal{O}(h) \tag{10}$$

When $u_{LR} \cong \bar{u}$, inequality (8) results in inequality (6). Inequality (6) can be regarded as satisfying the positively conservative condition for the internal energy approximately. Then, the parameter δ can be determined easily as

$$\delta = \min\left(\frac{\rho_{LR}}{|\sigma_1|}, \frac{1}{2}\right) \tag{11}$$

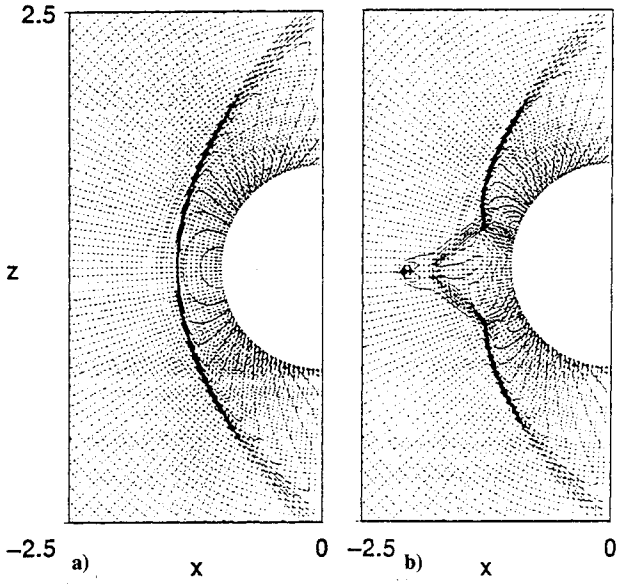

Fig. 1 Computed pressure contours of inviscid flowfield past a cylinder (M_∞ = 8): a) present scheme with Eq. (12) and b) present scheme without Eq. (12).

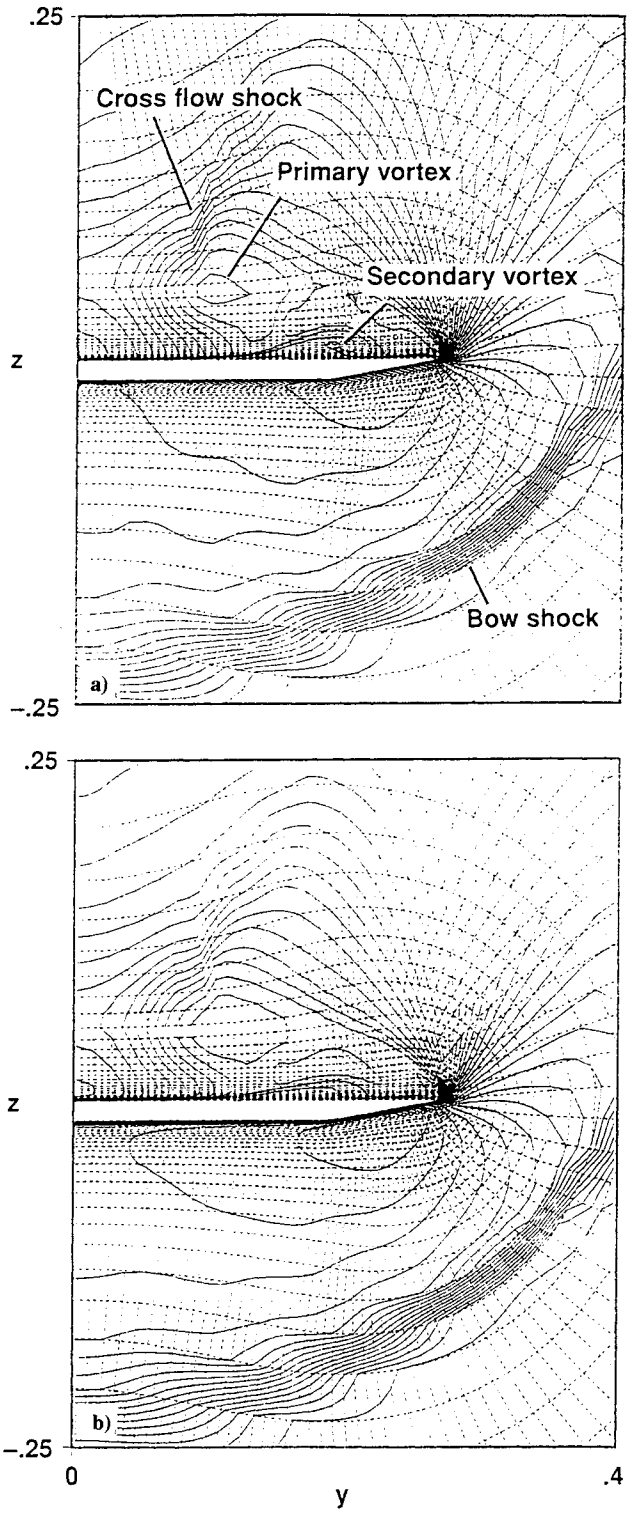

Fig. 2 Computed density contours of conical flowfield past a 75-deg delta wing (M_∞ = 2.8, α = 16 deg, and Re = 3.565 × 10^6): a) present scheme and b) HLLE scheme.

Equations (2), (5), and (11) give a new, approximate form of the modified HLLE scheme. Equation (11) indicates an interesting feature of the scheme. Because σ_1 represents a jump in entropy, it is zero for isentropic flows. Then, the present scheme results in the Roe scheme. In other words, the Roe scheme is positively conservative for isentropic flows. As the jump in entropy becomes large, the present scheme turns into the HLLE scheme.

When this scheme was extended to multidimensions by using dimensional splitting, the resulting scheme exhibited the carbuncle phenomenon (see Fig. 1). To overcome this problem, the parame-

ter δ was further reduced to obtain the HLLE scheme. Instead of introducing the HLLE switching function of Ref. 5, this was achieved by modifying Eq. (11). The pressure difference in σ_1 was replaced with

$$\sigma_1' = \Delta\rho - \Delta' p/\bar{c}^2 \tag{12a}$$

where

$$\Delta' p = \max(|\Delta p|, l_0 s/|\text{grad } p|) \cdot \text{sign}(\Delta p) \tag{12b}$$

and

$$s = \begin{cases} 1, & \text{for} \quad \boldsymbol{u} \cdot \text{grad } p > 0 \\ 0, & \text{for} \quad \boldsymbol{u} \cdot \text{grad } p < 0 \end{cases} \tag{12c}$$

and where l_0 is the length scale and is typically unity. The switch s turns on the HLLE scheme only at strong compression regions. The pressure gradient was evaluated at the left and right cells with central differencing, and the larger of the two values was used in Eq. (12).

Results

The one-dimensional scheme, Eqs. (2), (5), and (11), solved the shock-tube problems tested in Ref. 3 satisfactorily. Thus the results are not shown here. The following results were obtained from the multidimensional version of the present scheme derived from the standard dimensional splitting technique.

Figure 1 shows computed pressure contours for the carbuncle problem. The freestream Mach number is 8 and an inviscid ideal gas is assumed. This computation was performed on a 101 × 61 grid. Figure 1a shows the pressure contours obtained with the present scheme (first-order accurate) using Eqs. (2), (5), (11), and (12). The result indicates a stable bow shock wave. Figure 1b shows the corresponding plot without using Eq. (12). The carbuncle phenomenon appears here.

Figure 2 shows the computed density contours of the conical flowfield over a 75-deg delta wing at a freestream Mach number of 2.8, angle of attack of 16 deg, and a Reynolds number of 3.565×10^6. Laminar flow is assumed. The grid consists of 99 × 51 points. The present scheme was extended to third-order accuracy by using the MUSCL approach through the primitive variables.[6] The bow shock wave and the crossflow shock wave can be seen below and above the wing, respectively. The low density areas over the wing correspond to the primary and secondary vortices due to the flow separation at the leading edge. Figure 2a shows the result from the multidimensional version of the present scheme, while Fig. 2b shows the plots obtained from the HLLE scheme. The present result shows identical resolution to that of the Roe scheme. Without the switch, Eq. (12c), the present scheme became as dissipative as the HLLE scheme locally at the leading edge due to the strong expansion. As a result, the vortices were smeared out as shown in Fig. 2b. By implementing Eq. (12), the resolution of the resulting scheme remains as good as the Roe scheme, while the scheme is robust enough to prevent the carbuncle problem.

Acknowledgment

The first author's work was supported by NASA Grant NCC 2-605.

References

[1]Einfeldt, B., "On Godunov-Type Methods for Gas Dynamics," *SIAM Journal of Numerical Analysis*, Vol. 25, No. 2, April 1988, pp. 294–318.

[2]Einfeldt, B., Munz, C. D., Roe, P. L., and Sjögreen, B., "On Gudonov-Type Methods Near Low Densities," *Journal of Computational Physics*, Vol. 92, No. 2, 1991, pp. 273–295.

[3]Wada, Y., "An Improvement of the HLLEM Scheme and Its Extension to Chemically Reacting Flows," Second U.S. National Congress on Computational Mechanics, Washington, DC, Aug. 1993.

[4]Roe, P. L., "Approximate Riemann Solvers, Parameter Vectors, and Difference Scheme," *Journal of Computational Physics*, Vol. 43, No. 2, 1981, pp. 357–372.

[5]Quirk, J. J., "A Contribution to the Great Riemann Solver Debate," Institute for Computer Applications in Science and Engineering, ICASE Rept. 92-64, Nov. 1992.

[6]Obayashi, S., and Goorjian, P. M., "Improvements and Applications of a Streamwise Upwind Algorithm," AIAA Paper 89-1957, June 1989.

Numerical Investigation of Cylinder Wake Flow with a Rear Stagnation Jet

J. D. Mo and M. R. Duke Jr.*
Memphis State University, Memphis, Tennessee 38152

I. Introduction

WAKE flow characteristics behind a cylinder have been a topic of interest for years. Various means have been applied to attempt to eliminate the wake since the momentum deficit in the wake creates a considerable drag and an oscillating lateral force that causes mechanical vibrations on the cylinder. Upon visualization of the flow past a cylinder with a rear stagnation jet,[1,2] the flow appears fully attached as conventional inviscid flow does. Therefore, at first glance, it would be suspected that the form drag on the cylinder has been reduced to zero as predicted by inviscid flow theory. However, a detailed numerical simulation reveals that the form drag coefficient increases as the jet velocity increases. The mechanics of the increasing form drag will be addressed in this Note.

II. Computational Approach

A. Physical and Mathematical Model

The physical model for the numerical study is shown in Fig. 1. In this model, a stationary cylinder of radius R is placed in a uniform flow U_∞. A jet is located at the rear stagnation point with an area-averaged velocity V_j and jet direction parallel with the oncoming flow. For geometric simplicity, a polar coordinate (r, θ) system is adopted and is defined in Fig. 1.

The incompressible flow was treated as laminar because we were interested in Reynolds numbers, based on cylinder diameter, that were less than 2500. The Navier-Stokes equations in primitive variables are given as

$$\frac{\partial u_r}{\partial r} + \frac{u_r}{r} + \frac{\partial u_\theta}{r\partial\theta} = 0 \tag{1}$$

$$\frac{\partial u_r}{\partial t} + u_r\frac{\partial u_r}{\partial r} + u_\theta\frac{\partial u_r}{r\partial\theta} - \frac{u_\theta^2}{r} = -\frac{1}{\rho}\frac{\partial P}{\partial r} + \nu\left(\frac{\partial^2 u_r}{\partial r^2} + \frac{1}{r}\frac{\partial u_r}{\partial r} + \frac{1}{r^2}\frac{\partial^2 u_r}{\partial\theta^2} - \frac{2}{r^2}\frac{\partial u_\theta}{\partial\theta} - \frac{u_r}{r^2}\right) \tag{2a}$$

$$\frac{\partial u_\theta}{\partial t} + u_r\frac{\partial u_\theta}{\partial r} + u_\theta\frac{\partial u_\theta}{r\partial\theta} + \frac{u_r u_\theta}{r} = -\frac{1}{\rho}\frac{\partial P}{r\partial\theta} + \nu\left(\frac{\partial^2 u_\theta}{\partial r^2} + \frac{1}{r}\frac{\partial^2 u_\theta}{\partial r} + \frac{1}{r^2}\frac{\partial^2 u_\theta}{\partial\theta^2} + \frac{2}{r^2}\frac{\partial u_r}{\partial\theta} - \frac{u_\theta}{r^2}\right) \tag{2b}$$

Received June 29, 1993; presented as Paper 93-3274 at the AIAA 3rd Shear Flow Control Meeting, Orlando, FL, July 6–9, 1993; revision received Sept. 30, 1993; accepted for publication Oct. 26, 1993.

*Assistant Professor, Department of Mechanical Engineering. Member AIAA.

†Research Assistant, Department of Mechanical Engineering. Student Member AIAA.